Recent Developments of Commercially Fabricated Horn Antenna-Coupled Transition-Edge Sensor Bolometer Detectors for Next-Generation Cosmic Microwave Background Polarimetry Experiments

Aritoki Suzuki[1] · Elijah Kane[1,2] · Adrian T. Lee[1,2,3] · Tiffany Liu[1,2] · Christopher Raum[2,3] · Mario Renzullo[4] · Patrick Truitt[4] · John Vivalda[4] · Benjamin Westbrook[2,3] · Daniel Yohannes[4]

Abstract

We report on the successful fabrication of orthomode transducer-coupled transition-edge sensor (TES) bolometer arrays for cosmic microwave background (CMB) polarimetry experiments with the superconductor electronics fabrication facility at SEEQC Inc. Commercial microfabrication foundry could provide increase in detector fabrication throughput for a next-generation CMB experiment, CMB-S4, that would deploy approximately one order of magnitude more detectors than current CMB experiments. We also developed TES bolometers with two TESs in series that have two different superconducting temperatures (T_c) using a superconducting proximity effect between niobium (Nb) and aluminum-manganese (AlMn) alloy. We will discuss the motivation, design considerations, fabrication processes, test results, and how industrial detector fabrication could be a path to fabricate hundreds of detector wafers for future CMB polarimetry experiments and other experiments that require TESs and superconducting RF circuits.

Keywords Cosmic microwave background · TES bolometer · Fabrication · Technology transfer

✉ Aritoki Suzuki
asuzuki@lbl.gov

1   Physics Division, Lawrence Berkeley National Laboratory, Berkeley, CA 94720, USA

2   Department of Physics, University of California, Berkeley, CA 94720, USA

3   Radio Astronomy Laboratory, University of California, Berkeley, CA 94720, USA

4   SEEQC, Inc., Elmsford, NY 10523, USA

1 Introduction

Over the past few decades, scientists from around the world have made increasingly sensitive measurements of the cosmic microwave background (CMB) to study evolution and constituents of the universe. The CMB's spatial uniformity in its temperature and its black body spectrum has confirmed the hot big bang model of the universe. Detailed measurements of its small (10^{-5}) nonuniformity in temperature have led to tight constraints on the composition, geometry, and evolution of the universe. The CMB is also weakly polarized through Thomson scattering by free electrons in the early universe. This polarized CMB signal provides access to information that is inaccessible from the temperature anisotropy data. The CMB polarization signal will give us access to measure total mass of neutrinos, constrain effective number of relativistic species in the early universe, and probe whether early universe underwent inflationary expansion [1, 2].

To access the wealth of information encoded in the CMB polarization, scientists have deployed telescopes with low-temperature detectors designed to characterize the polarization state of the CMB. Detectors used by current CMB polarization experiments have an optical coupling element to couple CMB light onto microfabricated superconducting RF circuits on silicon wafers. The orthomode transducers separate two orthogonal linear polarization signals. The band pass filters also separate signals into two separate frequency bands. The signal is detected by transition-edge sensor (TES) bolometers that are cooled to 100 milli-Kelvin to 250 milli-Kelvin. CMB detectors have achieved a photon-noise limited noise performance where the detector's noise level is lower than a shot noise of incoming optical signal.

One way to improve the overall sensitivity of an experiment with photon-noise limited detectors is by increasing optical throughput by scaling up the number of detectors. Stage-2 CMB experiments deployed in the early 2010s with O(1000) detectors and have successfully detected B-mode polarization in the CMB that arises from weak gravitational lensing of E-mode polarization [3–7]. Stage-3 experiments deployed in the late 2010s with O(10,000) detectors and exciting results are being reported from these experiments [8–12].

The CMB community came together to work on the ultimate ground-based CMB experiment. This Stage-4 ground-based CMB experiment, CMB-S4, is being actively designed by teams of scientists and engineers. Current design for this next-generation CMB experiment calls for $\approx$500,000 detectors spread across 20 GHz to 300 GHz. The CMB-S4 is designed to measure $r \leq 0.001$ at 95% c.l., $\Delta N_{eff} < 0.06$ at 95% c.l., and produce a mm-wave legacy survey that will advance our understanding of galaxy clusters, gamma-ray bursts, and much more [2, 13, 14].

The CMB-S4 will require 432 science grade detector wafers fabricated over three years. This requirement is approximately an order of magnitude more detector wafers than that required for all Stage-3 experiments combined. As such, microfabrication, assembly, and testing of detector modules for CMB-S4 will be an immense task. In order to tackle the production throughput challenge for

next-generation CMB experiments, CMB-S4 projects are looking into fabricating detectors at multiple national laboratories, university laboratories, and industry partners. SEEQC Inc. and LBNL collaborated to expand CMB detector fabrication capability.

We initiated a technology transfer with SEEQC Inc. in late 2015, leading to the successful fabrication of an operational dual-polarization, dichroic sinuous antenna-coupled TES detector array on a 150-mm-diameter wafer. The performance of these earlier prototypes was reported in Suzuki et al. [15, 16]. Since then, the CMB-S4 project selected the horn-coupled orthomode transducer (OMT) technology as a baseline optical coupling technology for the CMB-S4 detector arrays. We made modification to sinuous antenna-coupled detector designs and fabrication process to fabricate the OMT-coupled detectors. In this report, we report on the design, fabrication, and characterization of OMT-coupled TES bolometer arrays fabricated at SEEQC Inc.

2 Design and Fabrication

We referred to fabrication process developed by NIST for the OMT-coupled TES bolometer detector array for Advanced ACTPol to develop OMT-coupled detector fabrication at SEEQC Inc. [17]. Figure 1 shows similarities and differences between lenslet-coupled detectors and horn-coupled detectors. Two types of detector technologies are fabricated in the same way except for how bulk silicon is removed to release membrane structures. The lenslet-coupled detector uses xenon difluoride (XeF2) gas process, and the horn-coupled detector uses Deep Reactive Ion Etch (DRIE) process. We based our fabrication processes on the mature lenslet-coupled detector fabrication process that we have developed [15, 16]. We used backside
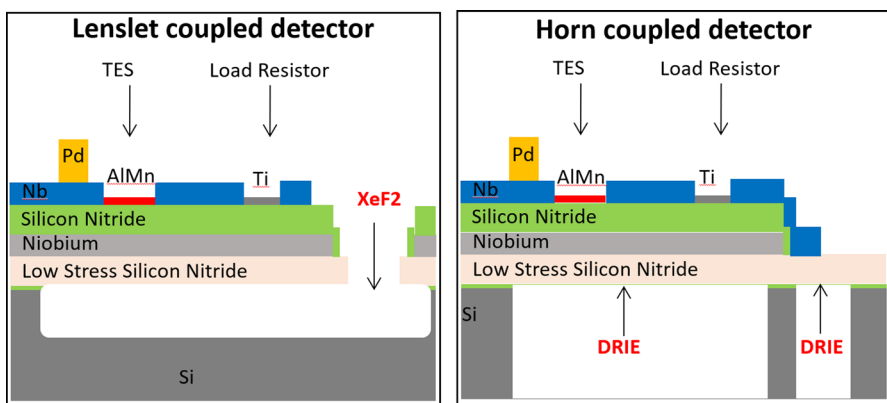

Fig. 1 (Color figure online) Comparison of layer stack between lenslet-coupled detector (left) versus horn-coupled detector (right). Layers and fabrication processes between two are same except for how bulk silicon is removed to release membrane structures. The lenslet-coupled detector uses xenon difluoride (XeF2) gas process, and the horn-coupled detector uses Deep Reactive Ion Etch (DRIE) process

through wafer etch to release silicon nitride membranes to fabricate the OMT-coupled detector array.

The detectors are fabricated on 150-mm silicon wafers that have low stress silicon nitride films and silicon oxide films pre-deposited by a commercial vendor. Next, a Nb/SiN/Nb trilayer is deposited with DC magnetron sputter and plasma enhanced chemical vapor deposition processes. Films are etched with reactive ion plasma to form superconducting circuits. Titanium and palladium films are used to form RF resistors and heat reservoirs for the TES bolometers, respectively. Both films are deposited with e-beam evaporation and patterned using a lift-off process. Manganese-doped aluminum (AlMn) is sputtered and then patterned with ion-milling to form the TES sensor, which is then passivated with a silicon nitride film to protect it from chemicals such as the photoresist developer. At the very end of the detector fabrication, silicon wafer is etched away from the backside to release membranes for OMT section and TES bolometers. For the membrane release process, the low stress nitride and silicon oxide films on the front side are first etched to expose the underlying silicon. Next, the entire front side of the wafer is covered with photoresist for protection. We then flip the wafer to lithograph DRIE features on backside of the wafer. We use RIE to etch away the low stress silicon nitride films and silicon oxide films to expose silicon on the back side. The bulk silicon is then removed from back of the wafer with the DRIE process. We use end point indicator to monitor the DRIE process to make sure the DRIE process do not etch through silicon nitride film on the front side.

After the DRIE etch, the wafer is immersed in acetone for eight hours to remove the photoresist. The remaining photoresist is removed with an oxygen plasma. Finally, the wafers are inspected and packaged for transportation.

The detector array for CMB-S4 is a hexagon diced out from a 150-mm silicon wafer. A large fraction of hexagonal edges of the detector array is diced using the DRIE process. However, we keep 200 micron wide bridges on sides and corners to connect central hexagonal region with rest of the wafer such that automatic wafer handling system of the DRIE system can move the wafer in and out of the process chamber. We use a dicing technique called stealth laser dicing, offered by GDSI Inc., to cut away these tabs to extract hexagonal wafers as shown in Fig. 2. Stealth laser dicing is a technique that uses a focused laser beam to break silicon crystals inside of silicon wafers. This technique allows wafer to be diced without disturbing fragile membranes on the wafer making it a suitable method to remove tabs post DRIE step.

3 Detector Performance

Since this fabrication cycle was the first TES bolometer designed and fabricated with DRIE release process at SEEQC Inc., our goal was to demonstrate design and fabrication of TES bolometers that operate at 100 milli-Kelvin with reasonable parameter values for a typical CMB experiment.

The characterization of fabricated detectors was performed in a dilution refrigerator cryostat at Lawrence Berkeley National Laboratory (LBNL). We did not have large detector holder to test the 130 mm hexagonal detector array; therefore,
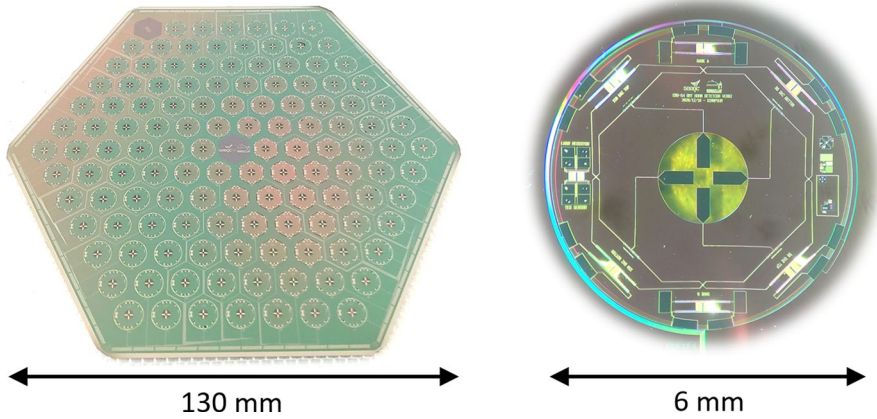
Fig. 2 (Color figure online) Photograph of OMT-coupled detector array (left) and zoomed in photograph of a pixel (right). Wafer size and pixel size are designed for CMB-S4 prototype mid-frequency (90 GHz/150 GHz) detector array

we tested pixels that were fabricated just outside of the hexagonal region. These pixels were diced off into small pieces during the laser dicing process that extracted hexagonal detector array. The chips were glued down to a copper plate with rubber cement. TES bolometers were mounted on the mixing chamber stage where we can vary bath temperature from 7 milli-Kelvin to 800 milli-Kelvin. TES bolometers were readout with the DC SQUID readout system from Quantum Design.
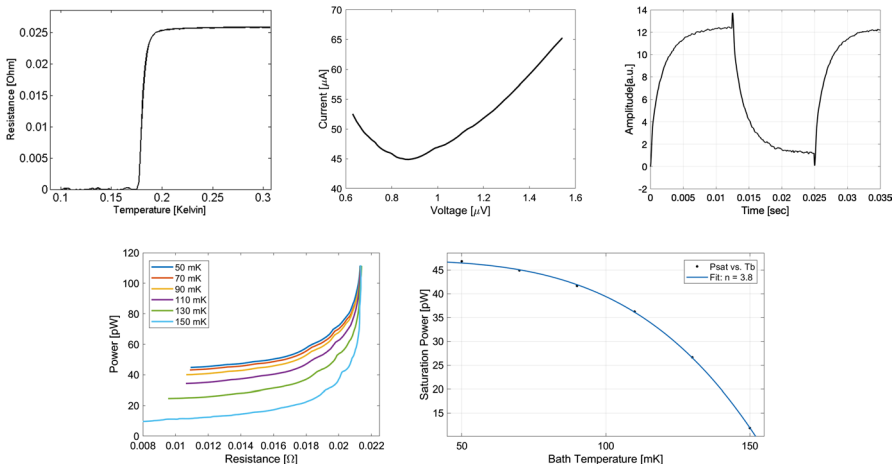

Fig. 3 (Color figure online) Plots from TES bolometer characterization. (Top left) Resistance of TES versus temperature. (Top middle) Current versus voltage curve at 100 milli-Kelvin base temperature. (Top right) Time constant measurement with stepped voltage bias. (Bottom left) Power versus resistance curves with various bath temperatures ranging from 50 milli-Kelvin to 150 milli-Kelvin. (Bottom right) Power versus bath temperature. Data was fitted with $P = k(T_c^n - T_b^n)$ with n = 3.8

Measurements of the TES bolometer's properties are shown in Fig. 3. Superconducting transition temperature (T_c) of the AlMn TES sensor had T_c of 180 milli-Kelvin. The TES bolometer exhibited expected IV behavior where current followed ohmic relationship above transition, and the IV followed constant power relationship, $I = P/V$, in superconducting transition state. We took multiple IV curves with various bath temperatures, and then we plotted power as a function of bath temperature. The data were fitted nicely with $P = k(T_c^n - T_b^n)$ where T_c is superconducting transition temperature and T_b is the bath temperature. Data fit well with thermal conductivity index $n = 3.8$ that is expected from a silicon nitride-based TES bolometer weak link with diffusive phonon thermal transport model. We measured electrical time constant of the TES bolometer by adding a small square wave on top of a DC voltage bias. TES bolometer exhibited expected exponential behavior with few milli-second time constant.

We have demonstrated successful operation of TES bolometers fabricated with a DRIE process membrane release.fa Furthermore, TES bolometer parameters are in reasonable ranges for CMB experiments. Collecting more statistics and fine tuning TES bolometer parameters to hit the specific target value will be the next goal. We did not have optical test setup and optical test components to test these devices optically. Our next goal is to test these pixels optically to characterize RF performance of horn-OMT-coupled detectors.

4 Dual T_c TES Bolometer

In our previous proceedings, we reported that T_c of AlMn TESs change as a function of distance between two niobium leads that make a contact to the TESs [16]. This is expected behavior as Nb modifies T_c of Nb/AlMn/Nb system via superconducting proximity effect. It has been used to tune T_c of TES sensors [18].

We used this phenomenon to build a dual Tc TES bolometer where TES with two different T_cs are connected in series. This design allows the same bolometer to be used in very different optical power loading conditions such as laboratory test versus CMB observation in field. This design has an advantage that we can achieve
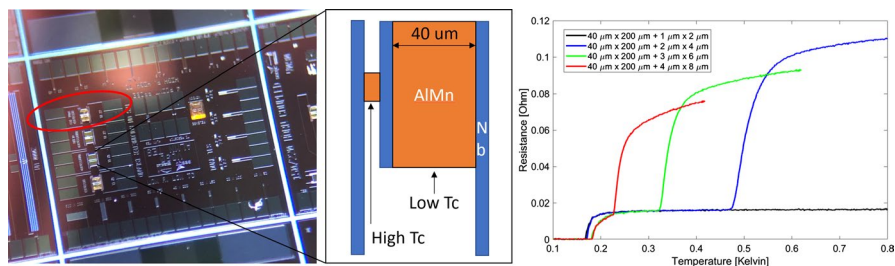

Fig. 4 (Color figure online) (Left) Photograph of test wafer fabricated for dual T_c TES characterization. (Center) Illustration of how dual T_c TES was designed. (Right) Measurement of resistance versus temperature of the dual T_c TES sensors. Different curves have different Nb spacings for the high T_c TES

different T_cs without changing fabrication process or adding extra metal layer to the fabrication.

As shown in Fig. 4, we connected to AlMn TESs with Nb leads with different distances between Nb leads. The low T_c TES had distance of 40 micron between two Nb leads, and for the high T_c TES, we varied Nb leads from 1 micron to 4 microns in a step of 1 micron to see how Nb/AlMn proximitization affect the T_c.

We fabricated a wafer using same fabrication processes as described above. We tested the temperature versus resistance relationship in the dilution refrigerator. As shown in Fig. 4, we were able to achieve dual transition TES and we were able change T_c of the high T_c TES.

5 Conclusion and Future Developments

We have successfully fabricated OMT-coupled TES detector array at SEEQC Inc. using DRIE process to remove bulk silicon. We have demonstrated operation of the TES bolometers from the chips that were fabricated using this process. We have also developed a way to achieve two TESs with two different T_cs connected in series without adding extra metal layers for simplicity.

Our next step is to characterize optical and RF properties of these pixels. Also, important future development is to establish a robust and repeatable fabrication process to meet performance requirement of CMB-S4 while maintaining high detector production throughput.

References

1. K.N. Abazajian et al., CMB-S4 Science Book, First Edition. arXiv: 1907.04473 [astro-ph.IM] (2016)
2. K. Abazajian et al., Cmb-s4 science case, reference design, and project plan (2019)
3. BICEP2 Collaboration et al., BICEP2. II. Experiment and three-year Data Set. APJ **792**, 62 (2014)
4. K. Array, BICEP2 Collaborations, et al., BICEP2/Keck Array VI: Improved constraints on cosmology and foregrounds when adding 95 GHz data from keck array. Phys. Rev. Lett. **116**, 031302 (2016)
5. J.E. Austermann et al., SPTpol: an instrument for CMB polarization measurements with the South Pole Telescope, in *Proceedings of the SPIE 8452, Millimeter, Submillimeter, and Far-Infrared Detectors and Instrumentation for Astronomy VI, 8452(84520E)* (2012)
6. M.D. Niemack et al., ACTPol: a polarization-sensitive receiver for the Atacama Cosmology Telescope, in *Millimeter, Submillimeter, and Far-Infrared Detectors and Instrumentation for Astronomy V, volume 7741 of SPIE*, p. 77411S (2010)
7. K. Arnold et al., The bolometric focal plane array of the POLARBEAR CMB experiment. Proc. SPIE **8452**, 84521D-84521D-12 (2012)
8. J.A. Grayson et al. BICEP3 performance overview and planned Keck Array upgrade. ArXiv e-prints (2016)

9.   B.A. Benson et al., SPT-3G: a next-generation cosmic microwave background polarization exper-
      iment on the South Pole telescope, in *Millimeter, Submillimeter, and Far-Infrared Detectors and
      Instrumentation for Astronomy VII, volume 9153 of SPIE*, p. 91531P (2014)
10. S.W. Henderson et al., Advanced ACTPol cryogenic detector arrays and readout. J. Low Temp.
      Phys. **184**, 772–779 (2016)
11. N. Stebor et al., The Simons Array CMB polarization experiment. SPIE **9914**, 99141H-99141H-9
      (2016)
12. D.T. Chuss et al., Cosmology large angular scale surveyor (CLASS) focal plane development. J.
      Low Temp. Phys. **184**(3), 759–764 (2016)
13. K. Abazajian et al., Cmb-s4 decadal survey APC white paper (2019)
14. S4 Collaboration et al. Cmb-s4: Forecasting constraints on primordial gravitational waves (2020)
15. A. Suzuki et al., Commercialization of micro-fabrication of antenna-coupled transition edge sensor
      bolometer detectors for studies of the cosmic microwave background. JLTP **193**(5), 744–751 (2018)
16. A. Suzuki et al., Commercially fabricated antenna-coupled transition edge sensor bolometer detec-
      tors for next-generation cosmic microwave background polarimetry experiment. JLTP **199**, 1158–
      1166 (2020)
17. S.M. Duff et al., Advanced actpol multichroic polarimeter array fabrication process for 150 mm
      wafers. JLTP **184**, 634–641 (2016)
18. T. Cecil et al., OMT-coupled CMB detector development at Argonne. IEEE Trans. Appl. Supercon-
      duct. **31**(5), 1–4 (2021)